Int. J. Solids Structures Vol. 29, No. 14/15, pp. 1737–1751, 1992
Printed in Great Britain.

0020-7683/92 $5.00 + .00
Pergamon Press plc

MULLINS' EFFECT AND THE STRAIN AMPLITUDE DEPENDENCE OF THE STORAGE MODULUS

SANJAY GOVINDJEE and JUAN C. SIMO
Division of Applied Mechanics, Department of Mechanical Engineering,
Stanford University, Stanford, CA 94305, U.S.A.

Abstract—A micromechanically based continuum damage model for carbon black filled elastomers exhibiting Mullin's effect is extended to incorporate viscous response within the framework of a theory of viscoelasticity which includes the classical BKZ model as a particular case and is not restricted to isotropy. The resulting model is shown to qualitatively predict the important effect of a strain amplitude dependent storage modulus even without the inclusion of healing effects. The proposed model for filled elastomers is shown to be well motivated from micromechanical considerations and suitable for large scale numerical simulations.

1. INTRODUCTION

Mullins' effect in carbon black filled elastomers is strain-induced stress softening. Under extensional loading, these materials undergo a strain-induced evolution of their microstructure that results in a change in their elastic properties. The physical system is a cross-linked elastomer matrix with a fine distribution of very small carbon particles. Typical particle sizes are on the order of 100 to 4700 Å in diameter (Blow and Hepburn, 1982, p. 208). The filler is added to the elastomer to enhance a wide variety of desirable material properties, viz. abrasion resistance, tear strength, and tensile strength; Mullins' effect is a side effect of the filler.

Phenomenologically Mullins' effect is most easily explained by considering an idealized quasi-static strain driven cyclic tension test (see Fig. 1). Quasi-static in the present context means that inertial and viscous effects are negligible; i.e. the loading is slow not only with respect to the inertial time scale but also with respect to the time scales of the viscous relaxation mechanisms in the elastomer. The material starts out in a virgin (undamaged) state (0). Upon initial loading to strain (1), path (a) defines the material behavior; upon subsequent unloading and loading between strain (1) and strain (0), path (b) defines the material behavior. So the material has experienced a permanent change in its properties due to the loading up to strain (1). If the strain load is increased beyond strain (1), path (a) is activated again in the region above strain (1). Assume the loading is increased to strain (2). Then, upon subsequent unloading and loading between strain (2) and strain (0), path (c) will define the material behavior. From a phenomenological viewpoint it is observed that in such materials there is a strain induced softening or damaging of the material; this is known as Mullins' effect. In a real experiment of this type, several other complications arise, which shall be addressed later in this introduction.

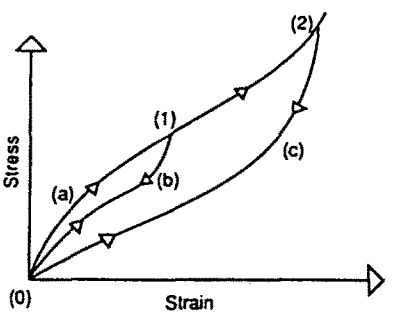

Fig. 1. Schematic of cyclic tension test demonstrating Mullins' effect.

In the work of Govindjee and Simo (1991a, b), the notion of the detachment of the elastomer matrix from the carbon particles as an explanation for Mullins' effect was developed into a quantitative micro-mechanically based continuum theory that was shown to agree well with some published experimental data for non-crystallizing materials; (the theory that has been proposed is predicated on the assumption that mechanisms that can be associated with the pure elastomer alone are not fundamental to Mullins' effect as has been advocated by other authors such as Harwood *et al.* (1965) or Harwood and Payne (1966a, b)). The micromechanical mechanism for Mullins' effect which is followed in this work was originally proposed in varying forms by Bueche (1960, 1961), Dannenberg (1974) and Rigbi (1980); but the version proposed by Bueche (1960) was chosen for simplicity. The difference between the concept of the direct interaction of the particles with the elastomer matrix and the somewhat more recent view of bound rubber with unbound rubber interaction (Hamed and Hatfield, 1989), can be resolved if a carbon black particle is understood as a composite system consisting of carbon and tightly bound rubber acting together.

There are, however, two important caveats to the theory previously presented by the authors.

(i) In a real application the loading rates are likely to be on or above the order of the relaxation rates of the elastomer network. Since such materials are typically highly cross-linked they exhibit only small amounts of viscoelastic behavior but nonetheless they do exhibit some viscoelastic behavior, and this must be accounted for in any theory that attempts to fully predict Mullins' effect. In the previous work these effects were ignored and the concentration was placed on the long-time behavior fundamental to understanding Mullins' effect. In this paper, an extension of the previous theory is presented that takes into account viscous relaxation effects in the elastomer matrix.

(ii) In the idealized experiment presented above, there is no notion of recovery of the stiffness of the material, i.e. healing. In reality, depending on the temperature, there can be healing effects, i.e. the reattachment of the elastomer matrix to the particles. For example, in a cross-linked poly(butadiene-co-styrene) (SBR) system with a silica type filler, Bueche (1961) has reported healing times on the order of many days for room temperature conditions, and times on the order of one day for elevated temperatures ($\approx 115\,^{\circ}C$). Healing will have a significant effect on materials in real applications where heat build up from viscoelastic hysteresis is large. Work on this aspect of the problem is deferred for later study.

In this work, the first point is circumvented by incorporating viscous effects into entropy elasticity models for polymer networks within a framework for finite strain viscoelasticity proposed in Simo (1987). This formulation of viscoelasticity is not restricted to isotropy and includes the isothermal version of the classical BKZ model (Bernstein *et al.*, 1963) as a particular case. Within this framework, relaxation processes in the material are described via stress-like convected internal variables, governed by dissipative evolution equations, and interpreted in the present context as the non-equilibrium interaction stresses between the polymer chains in the network. From a phenomenological standpoint, this class of viscoelastic models also admits a straightforward interpretation within the context of finite strain versions of classical rheological models.

In summary, the outline of the paper is as follows. First, a brief review of the non-viscous continuum model for Mullins' effect will be given in Section 2. Then, in Section 3 the addition of viscoelasticity to the model will be considered. Finally, in Section 4 some appealing aspects of the model will be exploited to produce efficient algorithms for performing numerical computations. Examples will be given in Section 5.

2. MICROMECHANICALLY BASED ELASTIC-DAMAGE MODEL

In this section a brief review of the details of the micromechanically motivated continuum damage model are given (see Govindjee and Simo (1991a and b) for a more extensive discussion of this model).

2.1. *Structure of the governing equations*

The model consists of an overall free energy density function W^∞ for the composite system that depends upon the volume average principal stretches λ_A and a scalar damage variable μ, i.e. isotropic damage. The superscript ∞ is a reminder that this function represents the long-time behavior of the material. The long-time free energy of the system is split into two parts and is given by:

$$W^\infty(\lambda_A, \mu) = (1-v_p)[W^\infty_{cc}(\lambda^m_A) + W^\infty_{pp}(\lambda^m_A, \mu)], \tag{1}$$

where W^∞_{cc} represents the free energy of the polymer chains that are cross-linked on both ends (given in this work as an Ogden rubber model: Ogden, 1984), W^∞_{pp} represents the free energy of the polymer chains that are attached on both ends to carbon black particles, v_p is the volume fraction of the carbon black particles, and λ^m_A are volume average stretches averaged over the polymer matrix volume. Polymer chains that do not fall into the two classes mentioned above are assumed to be accounted for by effective material properties. It is also noted that volume average strains on the system are the strains that are actually measured in an experimental setting.

The relation between the volume average strain quantities and the matrix volume average strain quantities is given by:

$$\mathbf{F} = \mathbf{RU}, \tag{2}$$

$$\mathbf{F}^m = \frac{\mathbf{R}(\mathbf{U}-v_p\mathbf{I})}{1-v_p}; \quad \text{for} \quad 0 \leqslant v_p < 1. \tag{3}$$

Equation (2) is the standard polar decomposition for the volume average deformation gradient, $\mathbf{F}$, in the material, where $\mathbf{R}$ is the rotation tensor and $\mathbf{U}$ is the right stretching tensor. Using this relation, eqn (3) gives the exact relation between $\mathbf{F}$ and the matrix volume average deformation gradient, $\mathbf{F}^m$, under the assumption of affinely rotating rigid particles in a C^0 deformation field, (where $\mathbf{I}$ is the identity). The affine rotation assumption for the particles is justified by the fact that the particles are large in size with respect to the crosslinks and are thus forced to rotate in an affine manner, whereas the crosslinks may move in a non-affine manner.

Since the material is assumed to be hyperelastic, stress quantities are given as partial derivatives of W^∞ with respect to their conjugate strain quantities. For example, volume average principal nominal stresses are defined by:

$$P_A = (1-v_p)\sum_{B=1}^{3}\left(\frac{\partial W^\infty_{cc}}{\partial \lambda^m_B} + \frac{\partial W^\infty_{pp}}{\partial \lambda^m_B}\right)\frac{\partial \lambda^m_B}{\partial \lambda_A}. \tag{4}$$

The last ingredients to the model are a damage criterion and an evolution equation for the damage variable μ. The damage criterion is given by

$$g = \max_{A=1,3}\{\lambda^m_A\} - \mu \leqslant 0, \tag{5}$$

and the evolution law by

$$\dot{\mu} = \gamma, \tag{6}$$

along with Kuhn–Tucker unilateral constraint conditions

$$\gamma \geqslant 0, \quad g \leqslant 0, \quad \gamma g = 0, \quad \gamma \dot{g} = 0. \tag{7}$$

Although the structure of eqns (5)–(7) can be formally motivated by appealing to a local principle of maximum dissipation, it is emphasized that these equations are, in fact, entirely

motivated from micromechanical considerations which take into account the changes taking place in the topology of the polymer network.

2.2. *Free energy functions*

To render tractable the constitutive model summarized in Section 2.1, an explicit expression for the free energy function W^{κ} must be given. It has been shown previously by the authors (see Govindjee and Simo, 1991b), that a suitable form of the free energy function is provided by the expression:

$$W^{\kappa}(\lambda_1, \lambda_2, \lambda_3, \mu) = U^{\kappa}(J) + \bar{W}^{\kappa}(\tilde{\lambda}_A, \mu) = U^{\kappa}(J) + (1 - c_p) \sum_{A=1}^{3} \tilde{w}(\tilde{\lambda}_A^m, \mu). \tag{8}$$

Here $U^{\kappa}(J)$ is a function that represents the macroscopic bulk response of the material which is nearly incompressible. For hyperelasticity formulated in principal stretches, this functional form of the free energy function is introduced in Simo and Taylor (1991) and interpreted as a penalty regularization of the stored energy function in the nearly incompressible range. Equation (8) is formulated in terms of the modified stretches

$$\tilde{\lambda}_A^m = \frac{\tilde{\lambda}_A - c_p}{1 - c_p}, \tag{9}$$

where $\tilde{\lambda}_A = J^{-1/3}\lambda_A$ are the modified principal stretches introduced by Flory (1961), and J is the Jacobian of the volume average deformation. Note that when the incompressibility constraint, $J \to 1$, is approached, then the average and matrix average modified stretches tend toward their unmodified values. The introduction of the modified stretches can be exploited in the design of effective algorithms which circumvent well-known numerical difficulties in the nearly incompressible limit; see Simo and Taylor (1991) for further elaboration. It should be noted that only the derivatives with respect to the first argument of the function $\tilde{w}(\cdot)$ appear in the governing equations; this derivative is given by

$$\partial_{\tilde{\lambda}_A^m} \tilde{w} = (1 + \chi(\tilde{\lambda}_A^m, \mu)) \sum_{p=1}^{3} m_p \tilde{\lambda}_A^{m(\alpha_p - 1)}, \tag{10}$$

where m_p and α_p are Ogden material parameters and

$$\chi(\lambda; \mu) = c_1(\mu)(\lambda - c_2(\mu))^2 + c_3(\mu). \tag{11}$$

In addition, the functions c_i $(i = 1, 2, 3)$ are defined by

$$c_i = k_i \exp\{(-1)^i \delta_i(\mu - 1)\} \quad (i = 1, 2, 3). \tag{12}$$

In eqn (12), $k_i \geqslant 0$ and $\delta_i \geqslant 0$ are dimensionless material parameters which are estimated from available experimental data. The function χ defines the relative strength of the polymer chains running between crosslinks to the polymer chains running between particles and the functions $c_i(\mu)$ indicate how χ evolves with progressing damage.

Explicitly, if one is interested in the volume average first Piola–Kirchhoff stress tensor, then relevant expression takes the form

$$\mathbf{P}(\mathbf{F}, \mu) = pJ\mathbf{F}^{-T} + \sum_{A=1}^{3} \left[\tilde{\lambda}_A \partial_{\tilde{\lambda}_A^m} \tilde{w}(\tilde{\lambda}_A^m, \mu) - \frac{1}{3} \sum_{B=1}^{3} \tilde{\lambda}_B \partial_{\tilde{\lambda}_B^m} \tilde{w}(\tilde{\lambda}_B^m, \mu) \right] \lambda_A^{-1} \mathbf{n}^{(A)} \otimes \mathbf{N}^{(A)}, \tag{13}$$

where $\mathbf{F} = \Sigma_{A=1}^{3} \lambda_A \mathbf{n}^{(A)} \otimes \mathbf{N}^{(A)}$ is the spectral decomposition of the deformation gradient and $p = \partial U^{\star}/\partial J$ is the hydrostatic pressure. Explicit form to the derivatives in eqn (13) is given by eqns (10)–(12) with the time evolution of the damage variable μ being given by the non-smooth eqns (5)–(7).

3. VISCOELASTIC MODEL

In this section, an extension of the time infinity (long-time) behavior model of Section 2 to "real" quasi-static loadings is considered. By "real" quasi-static loading, it is meant that only inertial effects will be neglected and that the viscous effects of polymer chain relaxation will be taken into account. As pointed out in the introduction, the extension proposed here exploits the specific model of finite strain viscoelasticity proposed in Simo (1987). In the spirit of existing theories of continuum viscoelasticity (see Truesdell and Noll, 1965, Section V for an overview), this model can be strictly justified only on phenomenological grounds. Nevertheless, the underlying structure can be motivated by the micromechanical considerations briefly described in what follows.

3.1. *Micromechanical motivation*

The micromechanical mechanism that gives rise to the phenomenologically observed viscoelastic response in polymers is presently understood as follows. When a crosslinked polymer is formed, the material starts out as a system of uncrosslinked polymer chains that are undergoing random conformational changes (Brownian motion). In this process, one can regard the polymer chains as being a tangled mass. If the material has been quiescent for a period of time, then the polymer chains, though tangled amongst each other, will be individually at equilibrium. Or in other words, there will be no bias along each polymer chain that will influence the direction of the random thermal fluctuations of the monomers. If at this time a set of permanent crosslinks is introduced into the system, then the entanglement of the polymer chains will become an invariant feature (assuming no chain scission) of the elastomer system topology and each chain will be forced to undergo its random thermal fluctuations in regions of space restricted by the permanent entanglements of the network. If a deformation is imposed on a macroscopic sample of such a crosslinked material, then the crosslinks and entanglement points will attempt to move in the mean in an affine manner with respect to the macroscopically imposed deformation. However, this motion will cause parts of chains to move from configurations of maximum probability; the process of moving back to a configuration of maximum probability will engender stress relaxation.

To be explicit, consider the case of a planar system and restrict attention to three entanglement points, enumerated (e_1, e_2, e_3), along the length of a given polymer chain, where there are n_1 chain segments between entanglements e_1 and e_2 and n_2 chain segments between entanglements e_2 and e_3. Further suppose that the vector that joins entanglements e_1 and e_2 lies in the 1 direction and that the vector that joins entanglements e_2 and e_3 lies in the 2 direction. Now consider an incompressible extensional deformation in the 1 direction so that there will be a contraction in the 2 direction. At the instant the deformation is imposed, a tensile force will build up along the arc length of the chain between e_1 and e_2 and a compressive force will build up along the arc length of the chain between e_2 and e_3. For equilibrium along the arc length of the entire chain, chain segments from between e_2 and e_3 will diffuse by a stress biased Brownian motion along the chain through e_2 into the region between e_1 and e_2. By this basic mechanism, stress relaxation is achieved in polymers.

Several authors have considered the calculation of constitutive models based on various forms of the mechanism described above. Representative of this approach are the work of Rouse (1953), Zimm (1956) and Doi and Edwards (1978a–c). Two main features underly these types of formulations. First, common to all these models is the estimation via micromechanical considerations of a discrete relaxation spectra with a history dependence which exhibits an exponential decay in time. Second, these models regard the polymer network surrounding a polymer chain as an equivalent medium providing an effective viscous

environment in which the Brownian motion of the chain segments must take place. These two key features are present in the approach described below which also employs the notion of a factorized memory kernel. The plausibility of a factorized memory kernel is justified on micromechanical grounds in the work of Doi and Edwards (1978c) which includes a number of references to experimental verification of this assumption in concentrated polymer systems.

3.2. *Continuum formulation*

Consider a representative volume sample $\mathcal{B}$ of polymer material, let $t > 0$ be the current time and denote by $\varphi_s : \mathcal{B} \to \mathbb{R}^3$, for $s \leqslant t$, the deformation history of $\mathcal{B}$ up to time t with deformation gradient $\mathbf{F}_s = D\varphi_s$. The deformation history is restricted by the standard condition that the right Cauchy–Green strain tensor

$$\mathbf{C}_s(X) = \mathbf{F}_s^T\mathbf{F}_s(X) \in \mathbb{M}^3_+, \quad \text{for} \quad \forall (X, s) \in \mathcal{B} \times [0, t], \tag{14}$$

where $\mathbb{M}^3_+$ is the set of 3×3 real symmetric matrices with positive determinant. Motivated by the preceding micromechanical considerations, $\mathcal{B}$ will be regarded as a continuum material possessing two distinctive features loosely characterized as follows:

(1) The constitutive response of the material for infinitely slow deformation histories (in the sense precisely described below) is *elastic*, possibly anisotropic (relative to the reference configuration $\mathcal{B}$) and characterized by an equilibrium elastic stored energy function $W^\infty : \mathbb{M}^3_+ \to \mathbb{R}$. (For notational simplicity, the damage argument μ will be suppressed throughout this section.)

(2) For arbitrary deformation histories the material response exhibits fading memory characterized by a discrete relaxation spectra with $N > 1$ retardation times τ^k, $(k = 1, 2, \ldots, N)$.

The first property reflects the elastic response of the polymer as characterized by the classical statistical models of entropy elasticity for the chains in the network, while the second property is the result of the viscous-like environment in which the Brownian motion of the chain segments takes place. The formulation described below incorporates these two effects in a continuum framework without precluding possible anisotropic response: a limitation present in the classical BKZ model.

3.2.1. *Mathematical model.* A relaxation process involves a trend to equilibrium in a mechanical system which, for the class of materials of interest here, is attained in the limit of infinite time. This notion can be recast in precise mathematical terms by assigning to each relaxation process in the material, with characteristic retardation time $\tau^k > 0$, a *non-equilibrium* stress denoted by $\mathbf{Q}^k_s$ $(k = 1, 2, \ldots, N)$ and governed by a dissipative evolution equation. Following a prescription dating back to Zaremba (see Truesdell and Noll, 1965, p. 45) to preclude restriction to isotropy and circumvent frame invariance issues, $\mathbf{Q}^k$ will be regarded as a convected stress tensor akin to the symmetric second Piola–Kirchhoff stress. The simplest dissipative evolution equation is defined by the linear *contractive* semi-group:

$$\left.\begin{aligned} \frac{\mathrm{d}}{\mathrm{d}s}\mathbf{Q}^k_s + \frac{1}{\tau^k}\mathbf{Q}^k_s &= \frac{\mathrm{d}}{\mathrm{d}s}[2\nabla W^k(\mathbf{C}_s)] \\ \mathbf{Q}^k_s|_{s=0} &= \mathbf{Q}^k_0 \end{aligned}\right\} \quad \text{in} \quad \mathcal{B} \times (0, t], \tag{15}$$

where $W^k : \mathbb{M}^3_+ \to \mathbb{R}$ is the instantaneous elastic stored energy in the material associated with the τ^k-relaxation process and ∇W^k indicates the derivative of $W^k(\cdot)$ with respect to its argument (the right Cauchy–Green tensor). Since the phenomenological relaxation effect is induced by a viscous environment induced by identical polymer chains, it will be assumed that

$$W^k(\mathbf{C}) = \beta^k_\infty W^\infty(\mathbf{C}) \quad \forall\, \mathbf{C} \in \mathbb{M}^3_+, \quad (k = 1, 2, \ldots, N), \tag{16}$$

where $\beta_\infty^k \in (0, \infty)$ are given non-dimensional constants associated with the retardation times τ^k. Further elaboration on the structure of (15) and (16) is given in Simo (1987).

Assuming instantaneous elastic response, the initial condition in (15) takes the form $\mathbf{Q}_0^k = 2\nabla W^k(\mathbf{C}_0)$; then, using the integrating factor $\exp[s/\tau^k]$, one obtains the explicit solution to the evolution equation as

$$\mathbf{Q}_t^k = \exp[-t/\tau^k]\beta_\infty^k[2\nabla W^\infty(\mathbf{C}_0)] + \int_{0^+}^{t} \beta_\infty^k \exp[-(t-s)/\tau^k]\frac{\mathrm{d}}{\mathrm{d}s}(2\nabla W^\infty(\mathbf{C}_s))\,\mathrm{d}s. \quad (17)$$

The formulation of the model is completed by prescribing the stress response at time t as a superposition of the equilibrium and non-equilibrium stress contributions. Explicitly, we define the second Piola–Kirchhoff stress as

$$\mathbf{S}_t = 2\nabla W^\infty(\mathbf{C}_t) + \sum_{k=1}^{N} \mathbf{Q}_t^k \quad \text{in} \quad \mathscr{B}. \quad (18)$$

Recalling the push-forward relation $\tau_t = \mathbf{F}_t\mathbf{S}_t\mathbf{F}_t^T$ between the spatial Kirchhoff stress and the second Piola–Kirchhoff stress, a straightforward manipulation yields the final result:

$$\tau_t = \mathbf{F}_t\left[g(t)2\nabla W^\infty(\mathbf{C}_0) + \int_{0^+}^{t} g(t-s)\frac{\mathrm{d}}{\mathrm{d}s}(2\nabla W^\infty(\mathbf{C}_s))\,\mathrm{d}s\right]\mathbf{F}_t^T \quad \text{in} \quad \mathscr{B}, \quad (19)$$

where $g(t) = 1 + \Sigma_{k=1}^{N} \beta_\infty^k \exp[-t/\tau^k]$ is a *normalized* relaxation function. Inspection of the convolution representation (19) reveals that the constitutive model is not restricted to isotropic response and remains properly invariant under superposed rigid body motions. The structure of (19) falls within the framework of the Green–Rivlin and Coleman–Noll theories (see Truesdell and Noll, 1965, p. 67).

3.2.2. *Rheological interpretation.* The significance of the dissipative evolution eqn (15) can be readily understood in the context of the linear rheological model depicted in Fig. 2. The one-dimensional linearized stored energy functions are given by $W^k = \frac{1}{2}E^k\varepsilon^2$ and $W^\infty = \frac{1}{2}E^\infty\varepsilon^2$, while the one-dimensional linear counterpart of eqn $(15)_1$ now reads

$$\dot{q}_s^k + \frac{1}{\tau^k}q_s^k = E^k\dot{\varepsilon}_s, \quad (k = 1, 2, \ldots, N), \quad (20)$$

where a superposed dot denotes time differentiation. Setting $\eta^k = E^k\tau^k$, the evolution equation (20) can be recast in the equivalent form

$$q_s^k = E^k[\varepsilon_s - \alpha_s^k] \quad \text{with} \quad \dot{\alpha}_s^k = q_s^k/\eta^k, \quad (21)$$

which describes the evolution of a Maxwell element with viscosity coefficient $\eta^k > 0$, spring

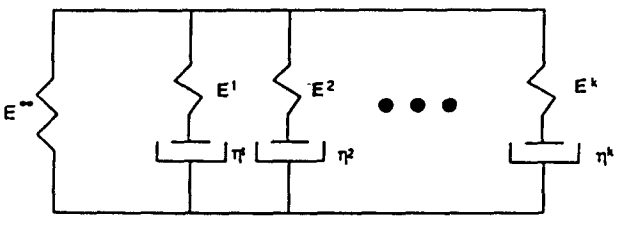

Fig. 2. One-dimensional rheological linear model consisting of an elastic element with elastic stiffness E^∞, connected in parallel with N Maxwell elements with viscosity coefficient η^k and elastic stiffness $E^k = \beta_\infty^k E^\infty$, respectively.

constant $E^k = \beta^k_r E^r$ and inelastic strain α^k, as shown in Fig. 2. In the same vein, the superposition relation (18) now reads $\sigma_t = E^\infty \varepsilon_t + \Sigma_{k=1}^N q_t^k$, and is interpreted merely as a statement of balance of forces in the mechanical device. In a sense, the continuum model outlined above represents a non-linear multi-dimensional generalization of the elementary situation described in Fig. 2.

3.2.3. *Independent bulk–shear viscous response.* Most polymer materials exhibit significantly different response in bulk and shear. For instance, rubber-like polymeric materials often exhibit nearly incompressible bulk response, while being capable of undergoing extremely large shear deformations. These experimental facts are incorporated into the basic viscoelastic constitutive model defined by (19) via a multiplicative decomposition of the deformation gradient, originally introduced by Flory (1961) in the restricted context of isotropic response and subsequently extended to the general setting and exploited within a variational framework in Simo *et al.* (1985) and Simo (1987). Specifically, for a given history of the deformation gradient, $\{\mathbf{F}_s(X): s < t\}$, at a point $X \in \mathcal{B}$, with Jacobian $J_s(X) = \det[\mathbf{F}_s(X)] > 0$, consider the local decomposition

$$\mathbf{F}_s(X) = J_s^{1/3} \bar{\mathbf{F}}_s(X) \Rightarrow \det[\bar{\mathbf{F}}_s(X)] = 1 \quad \forall (X, s) \in \mathcal{B} \times [0, t]. \tag{22}$$

The one-parameter family of linear maps $\{\bar{\mathbf{F}}_s: s \leqslant t\}$ defines the *volume preserving history* of the deformation gradient up to current time t. Now consider an uncoupled elastic stored energy function $W^r(\cdot)$ of the form

$$W^r(\mathbf{C}) = U^r(J) + \bar{W}^r(\bar{\mathbf{C}}) \quad \forall \mathbf{C} \in \mathbb{M}^3_+, \quad \text{where} \quad \bar{\mathbf{C}} = J^{-2/3}\mathbf{C}, \quad J^2 = \det[\mathbf{C}]. \tag{23}$$

Here, as before, $U^r(\cdot)$ is a convex function characterizing the bulk response of the material at equilibrium, while $\bar{W}^r$ defines the response of the material in shear, also at equilibrium. Note, however, that $W^r(\cdot)$ is a polyconvex function of $\mathbf{C} \in \mathbb{M}^3_+$ and is never convex in realistic models of elasticity; see e.g. Ciarlet (1988). By application of the chain rule one obtains the relation

$$\mathbf{S}^r = 2\nabla W^r(\mathbf{C}) = JU'(J)\mathbf{C}^{-1} + J^{-2/3}\,\mathrm{DEV}[2\nabla \bar{W}^r(\bar{\mathbf{C}})], \tag{24}$$

where $\mathbf{C} = \mathbf{F}^t\mathbf{F}$ is the right Cauchy Green strain tensor at equilibrium and $\mathrm{DEV}[\cdot] = (\cdot) - \frac{1}{3}\mathrm{trace}[(\cdot)\mathbf{C}]\mathbf{C}^{-1}$ gives the correct expression for the deviatoric part of a (contravariant) tensor in the convected description of elasticity. In fact, if $\tau^r = \mathbf{F}\mathbf{S}^r\mathbf{F}^t$ denotes the Kirchhoff stress tensor at equilibrium, relation (24) gives the following expression for the standard stress deviator in the spatial description:

$$\mathrm{dev}[\tau^r] = \bar{\mathbf{F}}[\mathrm{DEV}[2\nabla \bar{W}^r(\bar{\mathbf{C}})]]\bar{\mathbf{F}}^t \quad \text{where} \quad \bar{\mathbf{F}} = J^{-1/3}\mathbf{F}. \tag{25}$$

For a proof of relations (24) and (25) see Simo *et al.* (1985).

By exploiting the preceding framework it is possible to construct viscoelastic constitutive models possessing different viscoelastic response in bulk and shear. As an illustration, consider the formulation of a viscoelastic model exhibiting uncoupled response in bulk and shear, i.e. the viscoelastic counterpart of the uncoupled elastic model governed by the stored energy function (23). As before, the key idea is to regard the second Piola–Kirchhoff stress $\mathbf{S}_t$ at current time t as a superposition of equilibrium and non-equilibrium contributions of the form

$$\mathbf{S}_t = J_t\left[U^r(J_t) + \sum_{j=1}^M q_t^j\right]\mathbf{C}_t^{-1} + J_t^{-2/3}\,\mathrm{DEV}_t\left[2\nabla \bar{W}^r(\bar{\mathbf{C}}_t) + \sum_{k=1}^N \bar{\mathbf{Q}}_t^k\right]. \tag{26}$$

In the present context, the sets $\{\bar{\mathbf{Q}}_t^k: j = 1, 2, \ldots, N\}$ and $\{q_t^j: j = 1, 2, \ldots, M\}$ are interpreted as non-equilibrium stresses associated with the shear and bulk response of the

material. As in the preceding development, the evolution of these internal variables is governed by dissipative evolution equations. In particular, the appropriate counterpart of (15) becomes

$$\left.\begin{aligned} \frac{\mathrm{d}}{\mathrm{d}s}\bar{\mathbf{Q}}_s^k + \frac{1}{\bar{\tau}^k}\bar{\mathbf{Q}}_s^k &= \bar{\beta}_\infty^k \frac{\mathrm{d}}{\mathrm{d}s}[\mathrm{DEV}\,[2\nabla \bar{W}^\infty(\bar{\mathbf{C}}_s)]] \\ \bar{\mathbf{Q}}_s^k|_{s=0} &= \bar{\mathbf{Q}}_0^k \end{aligned}\right\} \quad \text{in} \quad \mathscr{B}\times(0,t], \tag{27}$$

where the constants $\bar{\tau}^k$ and $\bar{\beta}_\infty^k$, $(k = 1, 2, \ldots, N)$, define the characteristic retardation times and stored energy factors for the N relaxation processes associated with the volume preserving response of the material. Similarly, the simplest dissipative model for the internal variables q^j is furnished by the contractive semi-group

$$\left.\begin{aligned} \frac{\mathrm{d}}{\mathrm{d}s}q_s^j + \frac{1}{\tau^j}q_s^j &= \beta_\infty^j \frac{\mathrm{d}}{\mathrm{d}s}[U^{\infty\prime}(J_s)] \\ q_s^j|_{s=0} &= q_0^j \end{aligned}\right\} \quad \text{in} \quad \mathscr{B}\times(0,t], \tag{28}$$

where the constants τ^j and β_∞^k, $(j = 1, 2, \ldots, M)$, define the characteristic retardation times and stored energy factors for the M relaxation processes associated with the dilatational response of the material.

The preceding evolution equations admit a closed form solution in terms of a convolution integral involving the respective inhomogeneous terms in (27) and (28). Combining the foregoing results, the final constitutive relation for the Kirchhoff stress tensor at current time t can be expressed as a convolution integral involving the two normalized relaxation functions:

$$\bar{g}(t) = 1 + \sum_{k=1}^{N} \bar{\beta}_\infty^k \exp[-t/\bar{\tau}^k] \quad \text{and} \quad g(t) = 1 + \sum_{j=1}^{M} \beta_\infty^j \exp[-t/\tau^j], \tag{29}$$

which completely characterize the volume preserving the dilatational viscoelastic properties of the material.

Remarks.

(i) It can be shown that the preceding viscoelastic models are consistent with the Clausius–Duhem form of the second law of thermodynamics; see Simo (1987) and Govindjee (1991) for further details.

(ii) The class of viscoelastic models outlined above admits a number of possible generalizations. In particular, the simple dissipative evolution equations governing the response of the non-equilibrium stresses (internal variables) can be replaced by a suitable contractive semigroup. For instance, the general form of eqn (15) is

$$\left.\begin{aligned} \frac{\mathrm{d}}{\mathrm{d}s}\mathbf{Q}_s^k &= \mathbf{A}^k[\mathbf{Q}_s^k] + \frac{\mathrm{d}}{\mathrm{d}s}[2\nabla W^k(\mathbf{C}_s)] \\ \mathbf{Q}_s^k|_{s=0} &= \mathbf{Q}_0^k \end{aligned}\right\} \quad \text{in} \quad \mathscr{B}\times(0,t], \tag{30}$$

where $\mathbf{A}^k[\cdot]$ is the corresponding generator of a semigroup of contractions; see Dafermos (1976) for an explanation of this terminology. For the linear theory, the mathematical structure underlying models of this type has been examined in detail by Coleman and Mizel (1966) and Navarro (1978). It is felt, however, that the simple (and fairly classical) representations employed above often suffice for an adequate characterization of the viscoelastic response of the material.

(iii) The simplest example which illustrates the theory outlined above is furnished by an isotropic model with equilibrium stored energy function given in terms of principal

stretches, of the form

$$\bar{W}^{\alpha} = \hat{W}^{\alpha}(\tilde{\lambda}_1, \tilde{\lambda}_2, \tilde{\lambda}_3, \mu), \tag{31}$$

as already considered in the previous section. The functional structure of these models is ideally suited for incorporating viscoelastic effects in the damage model for filled rubbers proposed in Govindjee and Simo (1991a, b).

4. COMPUTATIONAL ASPECTS

The solution of the momentum balance equations over the time interval $\mathbb{I} = [0^+, t]$ in a computational setting is accomplished by an incremental procedure associated with a partition $\mathbb{I} = \cup_{n=1}^{L}[t_n, t_{n+1}]$, where $t_{L+1} \equiv t$. In a finite element setting, for a typical time subinterval $[t_n, t_{n+1}]$, one first assumes that μ_n and $\mathbf{Q}_n^k$ are given initial data and then solves for the deformation and the updated damage variable μ_{n+1} and internal variables $\mathbf{Q}_{n+1}^k$ for prescribed loading and boundary conditions. In the standard *strain driven* finite element setting, the balance equations are solved in an iterative manner. An estimate of the deformation field for time t_{n+1} is given and from it the damage and internal variables are calculated at time t_{n+1}. With these fields at hand the stresses at time t_{n+1} can be calculated and hence the balance of momentum can be checked. This process is repeated until convergence. What is needed in this loop is a means by which the damage evolution equations can be integrated (at each quadrature point of a typical finite element in the spatial discretization) from time t_n to t_{n+1} with μ_n as given initial data. Likewise for the internal variables, $\mathbf{Q}^k$, the evolution equations need to be integrated pointwise at the quadrature points from time t_n to t_{n+1} with $\mathbf{Q}_n^k$ as given initial data.

4.1. *Integration algorithm for damage variable*

Recalling that we are working within a strain driven setting, the evolution equations (5)–(7) for the damage may be integrated using the following consistent and unconditionally stable scheme.

0. Given $\{\tilde{\lambda}_A^m\}_{A=1}^3$ at a new time t_{n+1} and μ_n.
1. Sort $\{\tilde{\lambda}_A^m\}_{A=1}^3$ in decreasing order as a sub-sequence $\{\tilde{\lambda}_{A_I}^m\}_{I=1}^3$.
2. If $\tilde{\lambda}_{A_1}^m \leqslant \mu_n$, then no damage
   a. $\mu_{n+1} = \mu_n$.
3. Else damage taking place in at least one direction
   a. $\mu_{n+1} = \tilde{\lambda}_{A_1}^m$.
4. Endif.

Once the new damage variable has been determined, the corresponding long-time stress tensor is calculated from eqn (13). Note that the above algorithm possesses an exact linearization; see Govindjee and Simo (1991b). The exact linearization is of importance when using Newton and quasi-Newton methods to solve the balance equations in the iterative scheme mentioned above.

4.2. *Integration algorithm for internal variables*

For the internal variables the key aspect in the formulation of the discrete time stepping procedure is the evaluation of the convolution integral in eqn (17). For the infinitesimal theory, the key idea of evaluating convolution integrals via a recurrence relation is advanced in Herrmann and Peterson (1968) and Taylor *et al.* (1970), and extended to the nonlinear theory in Simo (1987). In the present context, the convolution integral is defined to be $\mathbf{H}^k$ and one is interested in evaluating $\mathbf{H}^k$ at time t_{n+1} when $\mathbf{H}_n^k = \mathbf{Q}_n^k - \exp[-t_n/\tau^k]\beta_\infty^k[2\nabla W^\infty(\mathbf{C}_0)]$ and φ_{n+1} are known. For the kernel in eqn (17), the following recurrence relation holds:

$$\begin{aligned}\mathbf{H}^k_{n+1} &= \int_{0^+}^{t_{n+1}} \beta^k_\infty \exp\left[-(t_n+\Delta t-s)/\tau^k\right] \frac{\mathrm{d}}{\mathrm{d}s}(2\nabla W^\infty(\mathbf{C}_s))\,\mathrm{d}s \\ &= \int_{0^+}^{t_n} \beta^k_\infty \exp\left[-\Delta t/\tau^k\right] \exp\left[-(t_n-s)/\tau^k\right] \frac{\mathrm{d}}{\mathrm{d}s}(2\nabla W^\infty(\mathbf{C}_s)) \\ &\quad + \int_{t_n}^{t_{n+1}} \beta^k_\infty \exp\left[-(t_{n+1}-s)/\tau^k\right] \frac{\mathrm{d}}{\mathrm{d}s}(2\nabla W^\infty(\mathbf{C}_s)) \\ &= \exp\left[-\Delta t/\tau^k\right]\mathbf{H}^k_n \\ &\quad + \int_{t_n}^{t_{n+1}} \beta^k_\infty \exp\left[-(t_{n+1}-s)/\tau^k\right] \frac{\mathrm{d}}{\mathrm{d}s}(2\nabla W^\infty(\mathbf{C}_s)).\end{aligned} \tag{32}$$

where $\Delta t = t_{n+1} - t_n$. Hence, $\mathbf{H}^k_{n+1}$ is determined in terms of the assumed known value $\mathbf{H}^k_n$ and an integral over the time step $[t_n, t_{n+1}]$. The integral can be estimated using the second order accurate midpoint rule to give the relation

$$\mathbf{H}^k_{n+1} = \exp\left[-\Delta t/\tau^k\right]\mathbf{H}^k_n + \exp\left[-\Delta t/2\tau^k\right]\{2\nabla W^\infty(\mathbf{C}_{n+1}) - 2\nabla W^\infty(\mathbf{C}_n)\}, \tag{33}$$

where the derivative at the midpoint has been linearly approximated. Note that this algorithm provides for unconditionally stable time stepping and the correct limits for large and vanishingly small times. Additionally, the algorithm may be exactly linearized for use in Newton and quasi-Newton global solution procedures.

5. NUMERICAL EXAMPLES

In this section, two examples are presented to demonstrate the qualitative performance of the viscoelastic damage model. In the first example, we wish to qualitatively reproduce the results for the storage modulus versus double strain amplitude in a forced vibration test. In the second example, we wish to demonstrate that the model and associated algorithms are suitable for large scale computations by running a moderately large finite element simulation.

5.1. *Forced vibration test*

In this test, the material (typically a cylindrical sample) is precompressed to a stretch of 0.9. Then, about this offset stretch, an oscillatory stretch is applied at some fixed frequency and amplitude. The double strain amplitude (DSA) in such tests refers to twice the amplitude of the deformation divided by the original sample length; the DSA is typically reported as a percentage. The storage modulus (Young's) is calculated as the real part of the complex modulus. These calculations are always made after the limit cycle has been reached. See Medalia (1978) or Brown (1979) for a discussion of such tests and various features of the dynamic properties of carbon black filled elastomers.

Due to the nonlinear nature of the material model, an analytic expression for the storage modulus in the conventional sense does not exist. So, to demonstrate the behavior of the model, a single stress point was driven about a precompression of 0.9 at a frequency of 2 Hz with incompressibility assumed. The trace of the engineering stress versus stretch was recorded and the calculation of the storage modulus was then performed in the same manner in which it is typically done in an experimental setting. The procedure is as follows. First, the loss angle is estimated as the arcsine of the ratio of the out-of-phase stress to the in-phase stress. Second, the magnitude of the complex modulus is obtained as the ratio of the in-phase peak-to-peak engineering stress amplitude to the DSA. Lastly, the storage modulus is given as the magnitude of the complex modulus multiplied by the cosine of the loss angle. The time infinity material properties in the simulation correspond to a poly-(styrene-co-butadiene) elastomer (SBR) with 50 phr S301 carbon black. The damage parameters are $k = \{5.6, 1.5, 6.9\}$ and $\delta = \{0.56, 0.21, 0.43\}$ and the Ogden parameters are

$\alpha = \{2.35, 7.03, 1.28\}$ and $m = \{1.11, 5.8 \times 10^{-4}, 0.73\}$ kg cm^{-2}; (see Govindjee and Simo, 1991b). Assume that the material has a relaxation spectrum defined by three relaxation times $\tau = \{0.5, 0.25, 0.125\}$ s where the constitutive parameters for these relaxation mechanisms are given as $\beta_\alpha = \{0.3, 0.1, 0.1\}$. These viscoelastic parameters are not meant to represent an actual material, but are merely given for illustrative purposes.

If the procedure spelled out above is followed, then we can obtain a plot of the storage modulus versus the DSA as shown in Fig. 3. The calculation was made using the algorithms in Section 4. Several remarks about Fig. 3 can be made:

(i) The basic characteristic feature of the storage modulus versus DSA plot has been replicated: namely, the drop in storage modulus with increasing DSA for a fixed value of the frequency of the loading.

(ii) In a real experiment, in the middle of the storage modulus drop there is an inflection point which is not present in Fig. 3. This inflection is due to temperature activated healing mechanisms in the system. As the amplitude is increased, the net heating of the sample increases and as a result the healing processes in the material are activated. As the material heals, it stiffens and hence the storage modulus is increased. This causes the inflection in the curve. Without the inclusion of healing effects in the model only qualitative results can be obtained from this theory. Healing is the subject of further research.

(iii) The upturn in the curve near 10% DSA is due to the non-linear elasticity of the elastomer itself.

(iv) If the problem is run without damage, then the drop in the storage modulus does not occur. The storage modulus is constant until a DSA of 10% and then increases rapidly due to the non-linearity of the elastomer. Hence, the damage is necessary for the effect to be seen.

5.2. *Finite element example*

In this example, we consider the finite element simulation of the extension and stress relaxation of a cube of material. The details of implementing damage models and viscoelastic models of the type proposed here in finite element codes have been given elsewhere and will not be repeated. Interested readers are directed to the works of Govindjee and Simo (1991b), Simo (1987) and Simo and Taylor (1991).

The problem we wish to consider is the uniaxial extension of a cube of material (8 ml) that is clamped on the top and bottom faces. The material is pulled in extension to a length

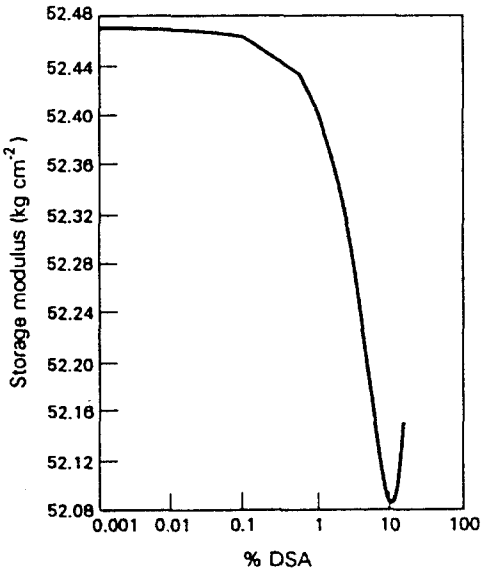

Fig. 3. Young's storage modulus versus % DSA for SBR with 50 phr S301 at 2.0 Hz.

of 2 ml in a time of 1 s in time steps of 0.1 s. The system is then held at the fixed extension and stress relaxation is allowed to occur. The material properties are the same as in the preceding example and once again, incompressibility is assumed. The incompressibility constraint is enforced via an Augmented Lagrangian scheme; see Simo and Taylor (1991).

Due to symmetry conditions only one-eighth of the geometry need be modeled. This sector on the cube was modeled with 1000 eight-node bricks with constant pressures, thus yielding a global finite element problem with 3289 degrees of freedom. This moderately large discretization of the geometry was chosen to demonstrate that such models can be used for doing large simulations with complicated three-dimensional stress states. Note that this problem develops complicated stress states due to the clamped end conditions and the damage. Figure 4 shows the iso-damage contours at full extension and Fig. 5 shows the 33 component (the loading is in the 3-direction) of the Cauchy stress at full extension before the material has started to relax. Figure 6 shows the total load on the sample as a function of time and shows the stress relaxation. Two remarks are in order:

(i) The ability of the material models to perform well in such situations is crucially linked to the fact that the integration algorithms for the viscoelastic and damage evolution can be exactly linearized. The exact linearization leads to asymptotically quadratic rates of global convergence when using Newton's method to solve the global finite element problem. Because of the asymptotically quadratic convergence, in a typical time step only 5 iterations were required to drive the residual norm down 9 orders of magnitude.

(ii) In the simulation, the natural logarithm of the Jacobian of the deformation is enforced to be $O(10^{-5})$. This large degree of incompressibility increases the numerical difficulty of the calculation and again points to the suitability of using such models in large numerical simulations.

6. CLOSURE

The main thrust of this work has been the formulation of a sound continuum viscoelastic damage model for filled polymers at finite strains, which is directly motivated from the micromechanics of this class of materials. The model gives good quantitative predictions

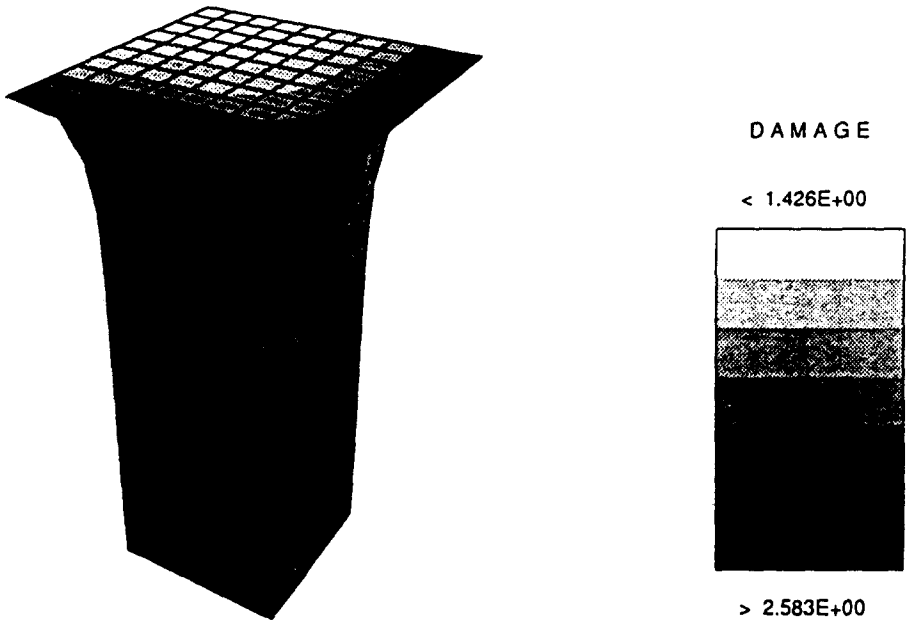

Fig. 4. Iso-damage contours at a time of 1 s.

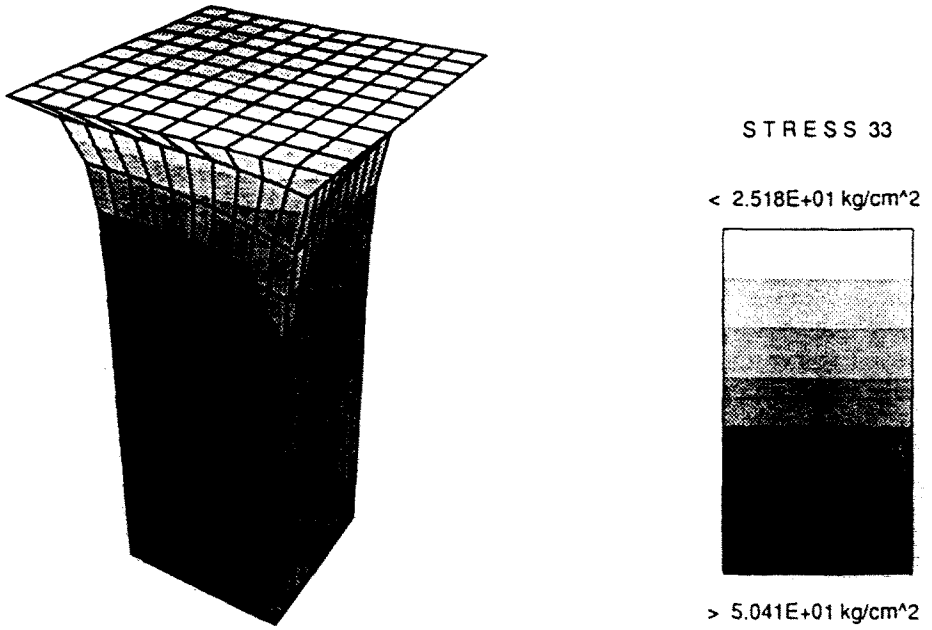

Fig. 5. Stress contours for the 33 components of the Cauchy stress at a time of 1 s.

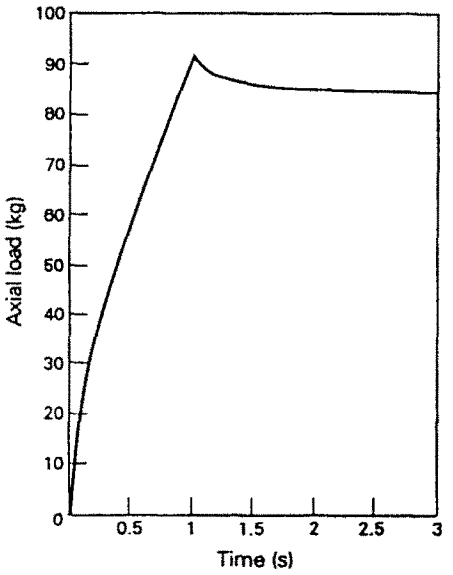

Fig. 6. Total load on cube versus time.

of the softening phenomenon exhibited by filled rubbers under deformation, known as Mullins' effect. Furthermore, the viscoelastic extension proposed in this paper is capable of predicting the reduction in storage modulus observed in cyclic tests with increasing double strain amplitude, as demonstrated by the results presented in Section 5.

In sharp contrast with a number of existing micromechanical and phenomenological models for filled polymers, the proposed approach is amenable to numerical analysis and suitable for large-scale simulations, as illustrated by the example presented in Section 5.

Acknowledgments—The authors wish to thank Dr R. L. Taylor of The University of California at Berkeley and Dr Ken Morman of the Ford Motor Company for their comments, interest and involvement in this work. Support for this research was provided by the Ford Motor Company and NSF under NSF Grant No. MSM 8657740 with Stanford University under the PYI program; this support is gratefully acknowledged.

REFERENCES

Bernstein, B., Kearsley, E. A. and Zapas, L. J. (1963). A study of stress relaxation with finite strain. *Trans. Soc. Rheo.* **7**, 391–409.

Blow, C. M. and Hepburn, C. (1982). *Rubber Technology and Manufacturing*. Butterworth, London.

Brown, R. P. (1979). *Physical Testing of Rubbers*. Applied Science, London.

Bueche, F. (1960). Molecular basis of the Mullins' effect. *J. Appl. Polym. Sci.* **4**, 107–114.

Bueche, F. (1961). Mullins' effect and rubber–filler interaction. *J. Appl. Polym. Sci.* **5**, 271–281.

Ciarlet, P. (1988). *Mathematical Elasticity*, Vol. I. *Three Dimensional Elasticity*, *Studies in Mathematics and its Applications*. North-Holland, Amsterdam.

Coleman, B. D. and Mizel, V. J. (1966). Norms and semigroups in the theory of fading memory. *Arch. Rat. Mech. Anal.* **23**, 87–123.

Dafermos, C. M. (1976). Contraction semigroups and trend to equilibrium in continuum mechanics. *Springer Lecture Notes in Mathematics* **503**, 295–306.

Dannenberg, E. M. (1974). The effects of surface chemical interactions on the properties of filler-reinforced rubbers. *Rubber Chem. Technol.* **48**, 410–444.

Doi, M. and Edwards, S. F. (1978a). Dynamics of concentrated polymer systems. Part 1. Brownian motion in the equilibrium state. *J. Chem. Soc. Faraday II* **74**, 1789–1801.

Doi, M. and Edwards, S. F. (1978b). Dynamics of concentrated polymer systems. Part 2. Molecular motion under flow. *J. Chem. Soc. Faraday II* **74**, 1802–1817.

Doi, M. and Edwards, S. F. (1978c). Dynamics of concentrated polymer systems. Part 3. The constitutive equation. *J. Chem. Soc. Faraday II* **74**, 1818–1832.

Flory, P. J. (1961). Thermodynamic relations for high elastic materials. *Trans. Faraday Soc.* **57**, 829–838.

Govindjee, S. and Simo, J. C. (1991a). A micro-mechanically based continuum damage model for carbon black-filled rubbers incorporating Mullins' effect. *J. Mech. Phys. Solids* **39**, 87–112.

Govindjee, S. and Simo, J. C. (1991b). Transition from micromechanics to computationally efficient phenomenology: carbon black filled rubbers incorporating Mullins' effect. *J. Mech. Phys. Solids* (in press).

Govindjee, S. (1991). Physical and numerical modelling in filled elastomeric systems. Ph.D. Dissertation, Division of Applied Mechanics, Stanford University.

Hamed, G. R. and Hatfield, S. (1989). On the role of bound rubber in carbon-black reinforcement. *Rubber Chem. Tech.* **62**, 143–156.

Harwood, J. A. C. and Payne, A. R. (1966a). Stress softening in natural rubber vulcanizates. Part III. Carbon black-filled vulcanizates. *J. Appl. Polym. Sci.* **10**, 315–324.

Harwood, J. A. C. and Payne, A. R. (1966b). Stress softening in natural rubber vulcanizates. Part IV. Unfilled vulcanizates. *J. Appl. Polym. Sci.* **10**, 1203–1211.

Harwood, J. A. C., Mullins, L. and Payne, A. R. (1965). Stress softening in natural rubber vulcanizates. Part II. Stress softening in pure gum and filler loaded rubbers. *J. Appl. Polym. Sci.* **9**, 3011–3021.

Herrmann, L. R. and Peterson, F. E. (1968). A numerical procedure for viscoelastic stress analysis. In *Proc. 7th Meeting of ICRPG Mechanical Behavior Working Group*, Orlando, Florida.

Medalia, A. I. (1978). Effect of carbon black on dynamic properties of rubber vulcanizates. *Rubber Chem. Tech.* **51**, 437–523.

Navarro, C. (1978). Asymptotic stability in linear thermovisco-elasticity. *J. Math. Anal. Appl.* **65**, 399–431.

Ogden, R. W. (1984). *Non-Linear Elastic Deformations*. Ellis Horwood, West Sussex.

Rigbi, Z. (1980). Reinforcement of rubber by carbon black. *Adv. Polym. Sci.* **36**, 21–68.

Rouse, P. E., Jr. (1953). A theory of the linear viscoelastic properties of dilute solutions of coiling polymers. *J. Chem. Phys.* **21**, 1272–1280.

Simo, J. C. (1987). On a fully three-dimensional finite-strain viscoelastic damage model: formulation and computational aspects. *Comp. Meth. Appl. Mech. Engng* **60**, 153–173.

Simo, J. C. and Taylor, R. L. (1991). Quasi-incompressible finite elasticity in principal stretches. Continuum basis and numerical algorithms. *Comp. Meth. Appl. Mech. Engng* **85**, 273–310.

Simo, J. C., Taylor, R. L. and Pister, K. S. (1985). Variational and projection methods for the volume constraint in finite deformation plasticity. *Comp. Meth. Appl. Mech. Engng* **51**, 177–208.

Taylor, R. L., Pister, K. S. and Goudreau, G. L. (1970). Thermomechanical analysis of viscoelastic solids. *Int. J. Numer. Meth. Engng* **2**, 45–59.

Truesdell, C. and Noll, W. (1965). The nonlinear field theories of mechanics. In *Handbuch der Physik* III/3 (Edited by S. Flugge). Springer, Berlin.

Zimm, B. H. (1956). Dynamics of polymer molecules in dilute solution. viscoelasticity, flow birefringence and dielectric loss. *J. Chem. Phys.* **24**, 269–278.